IEEE Access
Multidisciplinary ⋮ Rapid Review ⋮ Open Access Journal

Received 20 November 2022, accepted 29 November 2022, date of publication 6 December 2022,
date of current version 27 December 2022.

Digital Object Identifier 10.1109/ACCESS.2022.3227199

RESEARCH ARTICLE

Four-Element/Eight-Port MIMO Antenna System With Diversity and Desirable Radiation for Sub 6 GHz Modern 5G Smartphones

NASER OJAROUDI PARCHIN[1], (Senior Member, IEEE), AHMED S. I. AMAR[2], MOHAMMAD DARWISH[3], (Member, IEEE), KARIM H. MOUSSA[4], CHAN HWANG SEE[1], (Senior Member, IEEE), RAED A. ABD-ALHAMEED[5,6], (Senior Member, IEEE), NORAH MUHAMMAD ALWADAI[7], AND HEBA G. MOHAMED[8]

[1]School of Engineering and the Built Environment, Edinburgh Napier University, EH10 5DT Edinburgh, U.K.
[2]Department of Electronics and Communication, Air Defense College, Alexandria University, Alexandria 5424041, Egypt
[3]Radar Department, Military Technical College, Cairo 11865, Egypt
[4]School of Internet of Things, Xi'an Jiaotong–Liverpool University, Suzhou, Jiangsu 215123, China
[5]Bradford-Renduchintala Centre for Space AI, Faculty of Engineering and Informatics, University of Bradford, BD7 1DP Bradford, U.K.
[6]Department of Electrical Engineering, College of Engineering, University of Basrah, Basrah 61001, Iraq
[7]Department of Physics, College of Engineering, Princess Nourah Bint Abdulrahman University, Riyadh 11671, Saudi Arabia
[8]Department of Electrical Engineering, College of Engineering, Princess Nourah Bint Abdulrahman University, Riyadh 11671, Saudi Arabia

Corresponding author: Heba G. Mohamed (hegmohamed@pnu.edu.sa)

This work was supported by the Deputyship for Research and Innovation, Ministry of Education, Saudi Arabia, under Project RI-44-0421.

ABSTRACT In this manuscript, a multiple-input multiple-output (MIMO) antenna array system with identical compact antenna elements providing wide radiation and diversity function is introduced for sub 6 GHz fifth-generation (5G) cellular applications. The introduced design contains four pairs of miniaturized square-loop resonators with dual-polarization and independently coupled T-shaped feed lines which have been placed symmetrically at the edge corners of the smartphone mainboard with an overall size of 75 mm × 150 mm. Therefore, in total, the introduced array design encompasses four pairs of horizontally and vertically polarized resonators. The elements are very compact and utilize at 3.6 GHz, a potential 5G candidate band. In order to improve the frequency bandwidth and radiation coverage, a square slot has been placed and excited under each loop resonator. Desirable isolation has been observed for the adjacent elements without any decoupling structures. Therefore, they can be considered self-isolated elements. The presented smartphone antenna not only exhibits desirable radiation but also supports different polarizations at various sides of the printed circuit board (PCB). It exhibits good bandwidth of 400 MHz (3.4-3.8 GHz), high-gain patterns, improved radiation coverage, and low ECC/TARC (better than 0.004 and -30 dB at 3.6 GHz, respectively). Experimental measurements were conducted on an array manufactured on a standard smartphone board. The simulated properties of this MIMO array are compared with the measurements, and it is found that they are in good agreement. Furthermore, the introduced smartphone array offers adequate efficiency in both the user interface and components integrated into the device. As a result, it could be suitable for 5G handheld devices.

INDEX TERMS 5G, loop resonators, MIMO, mobile communications, smartphone antenna.

I. INTRODUCTION

Currently available wireless cellular systems (4G) cannot support future wireless communications that require high data transfer rates. As a result, the 5th generation (5G) of the mobile network have been established to meet these challenges and provide a variety of enhanced services on the internet of things (IoT), machine-to-machine (M2M), mobile broadband, massive MIMO, and ultra-reliable communications [1]. In order to acquire the main themes of

The associate editor coordinating the review of this manuscript and approving it for publication was Hassan Tariq Chattha.

5G networks, multiple antenna systems with an increased number of elements should be considered for future wireless networks. MIMO technology with multiple resonators can significantly amend the reliability function of the network [2], [3]. It is also an important parameter in increasing the wireless channel capacity by deploying equal multiple elements at the transmitter and the receiver ends without the need for additional power [4], [5]. MIMO system has been extensively used in 4G LTE and is a promising wireless technology to be included liberally in 5G. In addition, diversity schemes are considered to be a key component to combat fading and enhance wireless link reliability by sending the same signals through uncorrelated antennas [6].

High-efficient and low-profile antennas with sufficient operating bandwidth and mutual coupling characteristics are very suitable to be used in 5G terminals, especially in hand-portable devices [7], [8]. Microstrip antennas with low cost and ease of integration are appropriate to be applied in cellular applications due to the limited available space on smartphone boards [9]. Due to the restrictions on antenna size on smartphone boards, the compact microstrip-fed printed antennas with their planar forms, simple structures, and ease of integration with RF circuits, could be suitable candidates for smartphones [10]. Recently, many designs for smartphone antennas for 5G applications are provided at the frequency range below 6 GHz [11], [12], [13], [14], [15], [16], [17], [18], [19], [20], [21], [22]. However, these antenna arrays occupy wide spaces of the mainboard or use single-polarized resonators with non-planar structures and limited radiation coverage.

Therefore, we present here a new eight-port/four-element antenna array with miniaturized radiators and full radiation coverage. The single-element is composed of square-loop resonators with dual-polarization diversity which have been fed using independently coupled T-shaped feed lines. Due to its configuration and low-mutual function, it can be considered self-isolated. The elements are highly miniaturized and operate at 3.6 GHz in the sub-6-GHz 5G spectrum supporting the frequency of 3.4 to 3.8 GHz. The presented antenna system is designed using the commercially available CST software package [23]. In addition, the proposed MIMO design is implemented, and its characteristics are measured. To confirm the accuracy of the designed antenna performances, the measurement results are carried out and have been compared to the electromagnetic simulations. Compared with the recently intruded MIMO antenna, it possesses several unique features such as good isolation, excellent radiation coverage, low ECC/TARC, and sufficient efficiencies. The fundamental characteristics of the single radiator and its array design are elaborated in the following. It should be noted that using modified ground planes (with slot and slit cuts) is a very common method in smartphone antenna design [24], [25], [26]. It might slightly reduce the remaining space for the screen LCD but could provide some attractive features. In addition, in order to represent the capability of the proposed design for full-ground plane applications [27], a modified design of the MIMO antenna with the full-ground plane (whole metal plate) is discussed in section VI. In this section, the slots are not considered. The results show sufficient S-parameters and gain results. However, compared to the design with slots in the ground, it has limited radiation coverage which mainly covers the top side of the smartphone PCB. It also exhibits lower impedance bandwidth and also gain-levels. Therefore, dual-polarized design with the modified ground plane was used.

II. SINGLE-ELEMENT ANTENNA PROPERTIES

The schematic diagram of the design is represented in Fig. 1. It consists of a square-ring resonator with a slotted ground plane on the top and back layers of the dielectric, respectively. It is established by two coupled feeding structures with 50-Ohm T-shaped feeding lines. The antenna was arranged on a 1.6 mm FR4 with 4.3 permittivity and a loss tangent of 0.025.

The design parameters of the single resonator and the MIMO array (in mm) are listed in Table 1.

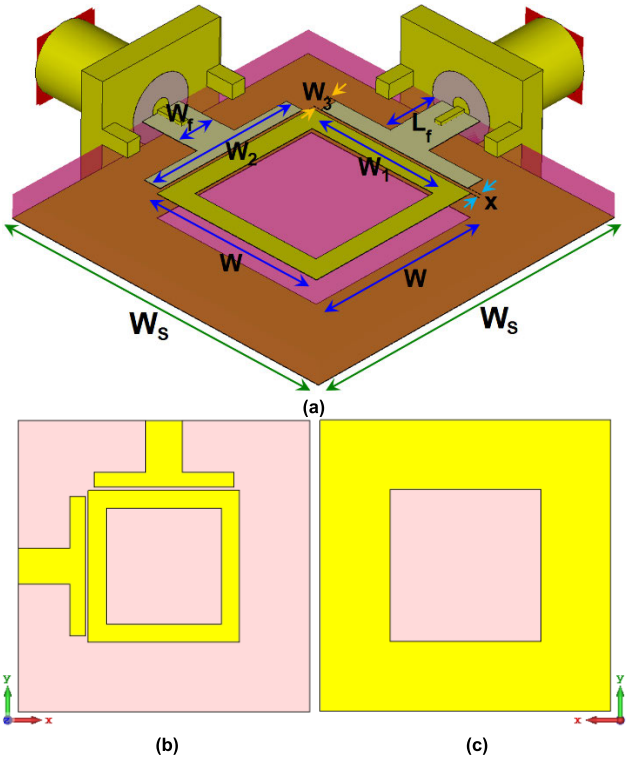

FIGURE 1. (a) Side-view, (b) top-layer, and (c) bottom-layer of the proposed dual-polarized antenna element.

In order to design a microstrip-fed patch antenna, three parameters are essential: operating frequency (f_0), thickness, and dielectric constant. [28]. The patch's width can be specified by:

$$W_{sub} = \frac{C}{2f_0\sqrt{\frac{(\varepsilon_r+1)}{2}}} \quad (1)$$

TABLE 1. The values of the designs.

Parameter	Value (mm)
W_S	24
W_{sub}	75
L_{sub}	150
h_{sub}	1.6
W	12.5
W_1	9.5
W_2	11.5
W_3	1.9
W_f	3
L_f	0.2
x	0.25

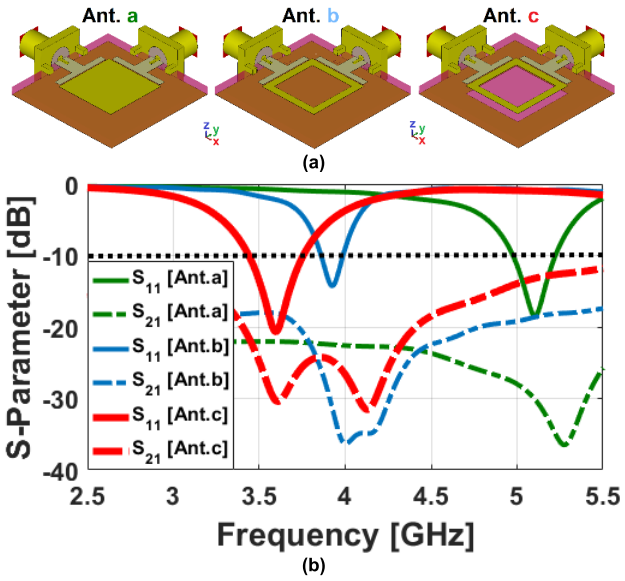

FIGURE 2. (a) Evaluation and (b) S-parameter results of the antennas (a-c).

where ε_r, f_0, and C are the dielectric constant (permittivity) of the substrate, the desired resonant frequency, and the Speed of light, respectively. The antenna's effective permittivity (εr_{eff}) can be calculated:

$$\varepsilon_{eff} = \frac{(\varepsilon_r + 1)}{2} + \frac{(\varepsilon_r - 1)}{2}\left[1 + 12\frac{h_{sub}}{W_{sub}}\right]^{-\frac{1}{2}} \quad (2)$$

The size of the antenna patch along its length have been extended on each end by a distance of ΔL, that can be given by:

$$\Delta L = 0.421 h_{sub}\frac{\left(\varepsilon_{eff} + 0.3\right)\left(\frac{W_{sub}}{h_{sub}} + 0.264\right)}{\left(\varepsilon_{eff} - 0.258\right)\left(\frac{W_{sub}}{h_{sub}} + 0.8\right)} \quad (3)$$

where h_{sub} is the thickness of the substrate and W_{sub} is the itse width. In addition, the effective length of resonator is:

$$L_{eff} = \frac{C}{2f\sqrt{\varepsilon}_{reff}} \quad (4)$$

By modifying the antenna radiating from the square patch to the square-ring loop, the optimized length $L_{resonance}$ is set to resonate at $0.25\lambda_{resonance}$, where $L_{resonance} = 2W\text{-}W_1$ corresponds to the target resonance frequency (3.6 GHz).

The presented antenna has undergone a few evolutions before it was miniaturized. Various configuration and S-parameter results of the basic patch antenna with a square-patch radiator (Ant. a), the design with a ring patch resonator (Ant. b), and the introduced design (Ant. c) are represented and compared in Figs. 2 (a) and (b). As can be clearly observed, the main resonance of the basic antenna occurs at 5.15 GHz, while by changing it to the form of a loop-ring, the length of the resonator increases, therefore the antenna can operate at the lower frequency (3.9 GHz). It can be observed that the loop patch (with a full ground plane) is the main radiator of the proposed design and can be easily modified to operate at the desired band. However, in order to improve the isolation, impedance bandwidth and also the radiation coverage, a square-shaped slot has been placed at the ground plane. Therefore, by placing a square-shaped slot in the back layer, the design operates at the target frequency band with well-defined matching and improved bandwidth (3.4-3.8 GHz). In addition, high isolation and low coupling between the antenna ports have been discovered at the desired band.

The proposed dual-polarized antenna was fed using a pair of coupled T-shaped feed lines which provide good impedance matching. Figure 3 discusses the antenna performances for different feeding methods. Different types of feeding including connected rectangular, coupled rectangular, and coupled T-shaped feed lines are shown in Fig. 3 (a) and their performances are discussed in Fig. 3 (b). As clearly shown, the antenna with a pair of connected rectangular feedlines acts as a band-stop filtering element without antenna radiation. While by using the coupled rectangular, the antenna creates weak radiation at the target frequency. Finally, by using the proposed coupled T-shaped feed lines, well-defined performance with wide bandwidth and low mutual coupling has been observed.

The frequency response of the suggested double-fed antenna can be easily changed and tuned to the desired band, by changing the design parameters. In addition, the isolation and impedance bandwidth of the design can be modified [29], [30]. One of the main parameters relates to the length of the square ring (W). The simulated S_{11} curves of the dual-polarized design with different sizes of W are represented in Fig. 4 (a): when the length of the ring increases from 7.5 mm to 11.5 mm, the resonance frequency can be tuned from 3.7 to 3.4 GHz while maintaining sufficient

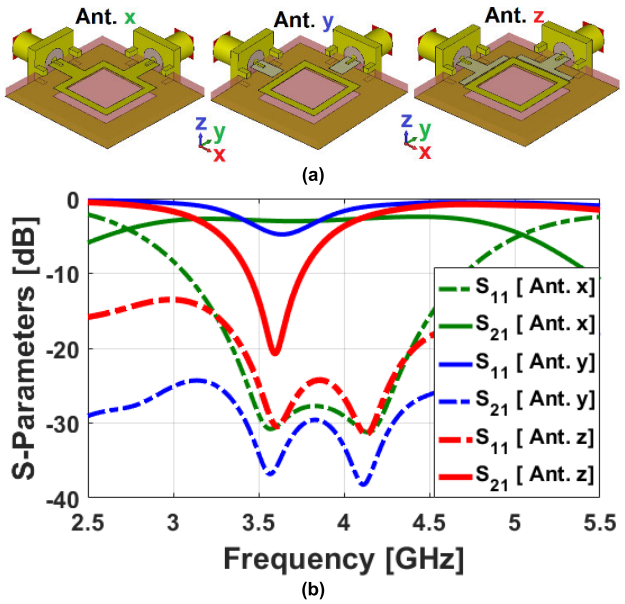

FIGURE 3. (a) Evaluation and (b) S-parameter results of the antennas (x-z).

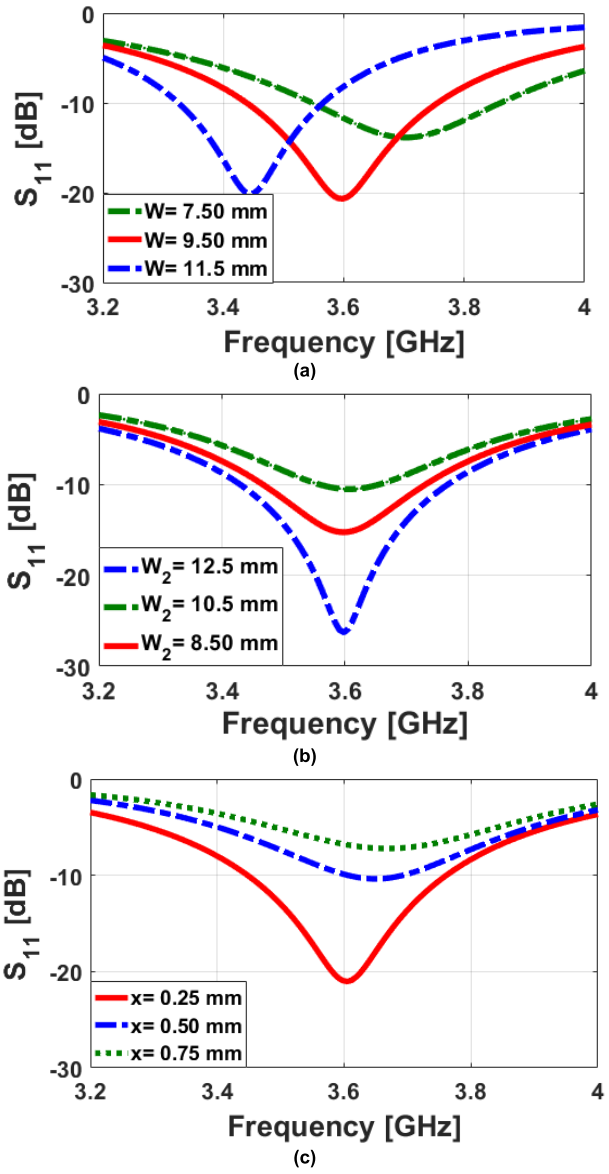

FIGURE 4. S_{11} results for different values of (a) W, (b) W_2, and (c) x.

impedance matching. The antenna element is fed by a pair of independent coupled feeding structures, whose size can affect the antenna performance. The S_{11} characteristic of the suggested antenna design with different values of W_2 is shown in Fig. 4 (b). As seen, the isolation of the antenna frequency response of the antenna can be changed for different values of the coupled feeding structures.

Another important design parameter is the coupling distance between the feedlines and the main radiator (x) which plays a critical part in the impedance matching and antenna bandwidth. The antenna S_{11} results for different values of x are shown in Fig. 4 (c). It is evident for x= 0.25mm, the antenna provides sufficient bandwidth with a return loss less than -20, covering the 3.4-3.8 GHz 5G band.

Figures 5 (a) and (b) depict the surface current distributions and densities at the resonating frequency of 2.6 GHz in the top/back layers, respectively. As shown, there is a significant distribution of currents around the resonator. In addition, the embedded slot appeared to be highly active, with surface currents flowing in opposite directions for different ports [31], [32].

Figures 6 (a) and (b) plot the radiation patterns (Phi) for two different ports. It can be observed that the antenna provides identical radiations and more than 3.15 dB IEEE gain. As shown, the antenna exhibits similar performance with a 90° difference and dual polarizations due to the feeding ports. The efficiency properties and maximum gain results of the suggested design are represented in Fig. 6 (b). It can be seen from the figure that each antenna has a high radiation efficiency of more than 80%. It also exhibits better than 70% total efficiency at the desired bandwidth. Moreover, as represented in Fig. 6 (c), for the range of 3.4-3.8 GHz, the obtained efficiencies are quite acceptable for MIMO operation [33]. Furthermore, the maximum gain property of the antenna varies from 3 to 3.5 dBi. The prototype sample of the suggested antenna design has been fabricated and tested. Figure 7 depicts the fabricated sample along with its measured S parameters. It is evident from Fig. 7 (b) that the sample works properly and is quite well-aligned with simulations. As evident, the fabricated antenna is operating at the frequency range of 3.4-3.8 GHz and provides well-defined mutual coupling, less than −30 dB. It is worth noting that for −6 dB, better than 600 MHz bandwidth is obtained.

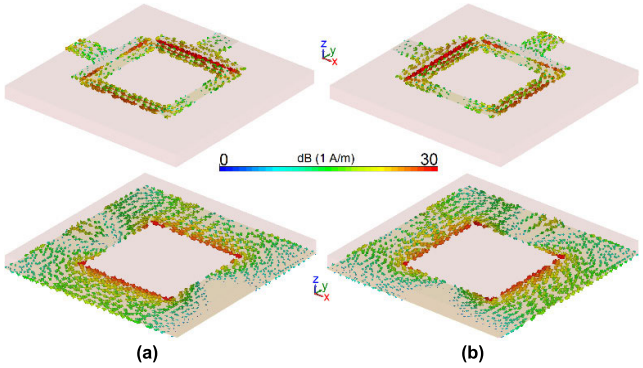

FIGURE 5. Current distributions at 3.6 GHz for (a) 1st port and (b) 2nd port.

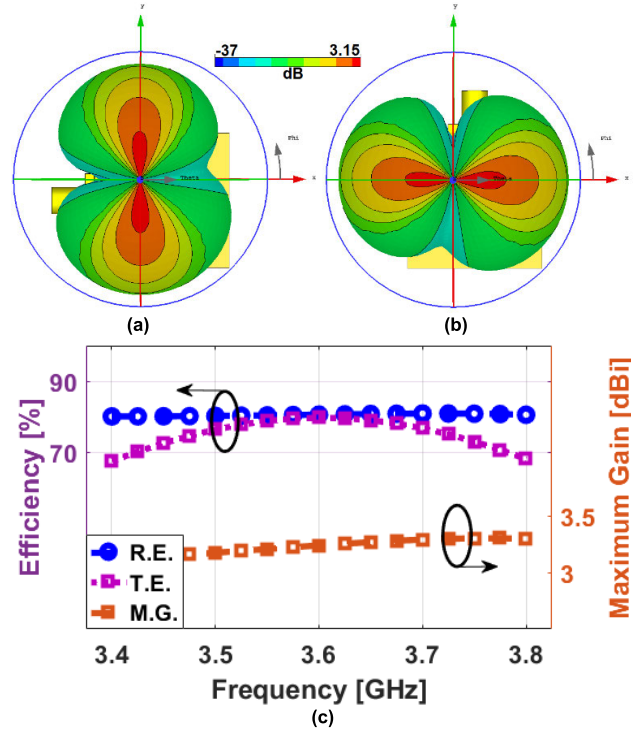

FIGURE 6. 3D-radiation (Phi) for dual-polarization from (a) 1st port, (b) 2nd port, and (c) the efficiency/max. gain characteristics versus the antenna operation band.

III. CHARACTERISTICS OF MIMO ANTENNA DESIGN

The perspective 3D side view of the introduced MIMO smartphone antenna design is plotted in Fig. 8 (a). In addition, the front and back layers are represented in Figs. 8 (b) and (c), respectively. As shown, the structural configuration of the introduced multi-feed antenna system is quite straightforward and simple. The overall size is 75 × 150 mm2 and it has 8 × 8 square-ring loop antennas with coupled T-shaped microstrip feedings. It should be noted that multiple similar antenna elements have been deployed at four edges of the board. Employing the suggested resonators not only improves the frequency response and matching characteristics but also exhibits symmetrical radiations covering the top/bottom of

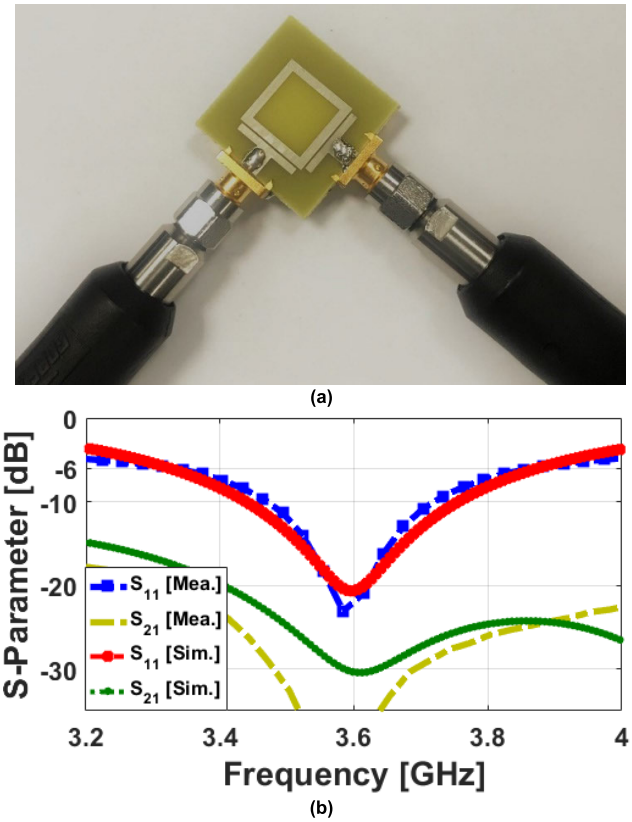

FIGURE 7. (a) Fabricated sample connected to the coaxial cables and (b) simulated/measured S-parameters (S_{11}, S_{21}).

the board [34]. The S-parameters of the designed antenna array shown in Fig. 9 indicates that the antenna elements have similar performance and provide high matching offering better than -20 dB reflection coefficients (S_{nn}) at the desired frequency of 3.6 GHz. Furthermore, as plotted in Fig. 8 (b), the elements have good isolation with mutual coupling (S_{nm}) less than -17 dB.

As mentioned earlier, employing the slots in the ground plane not only increase the covering spectrum of the antenna resonators but also could improve the radiation of the antenna and provide wide and desirable coverage. Figure 10 shows the current distributions of Antennas 1 & 2 at 3.6 GHz in both front and back layers.

It is shown that the currents are significantly distributed around the loop element. Moreover, the inserted slot has appeared active with the surface currents flowing contrary for different ports [35], [36].

Figure 11 represents and compares the antenna radiation with and without the employed square slot. As seen in Fig. 11 (a), the antenna without the square slot mainly supports the top region of the substrate while, by placing the slot, quasi-symmetrical broadside radiation (Fig. 11 (b)) can be achieved which leads to improved radiation coverage suitable for MIMO smartphone communications. For a better understanding, the 3D radiation patterns of the multiple antenna elements with their gain values are shown in Fig. 12. As seen,

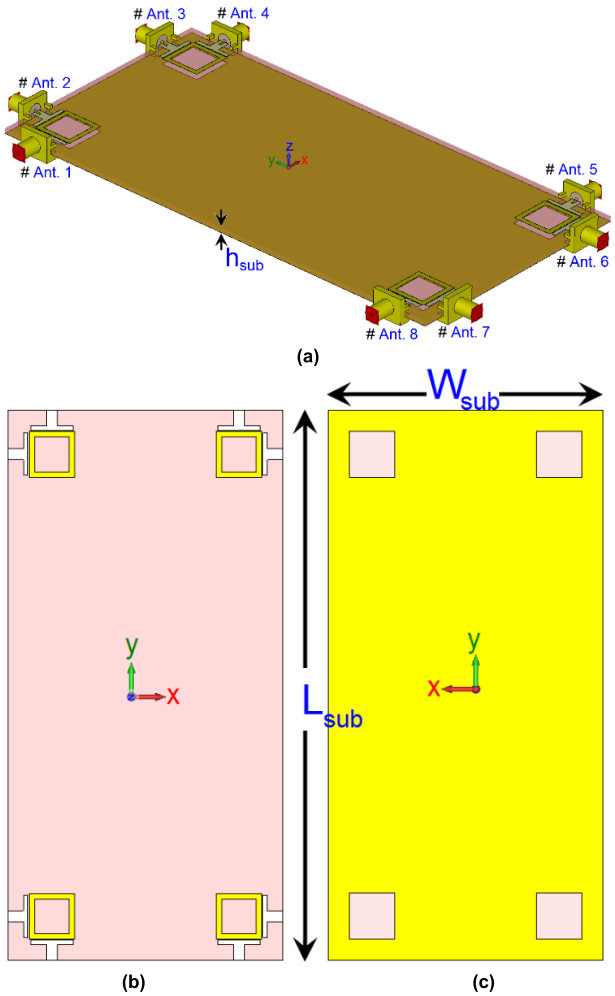

FIGURE 8. (a) Side, (b) front, and (c) back views of the design.

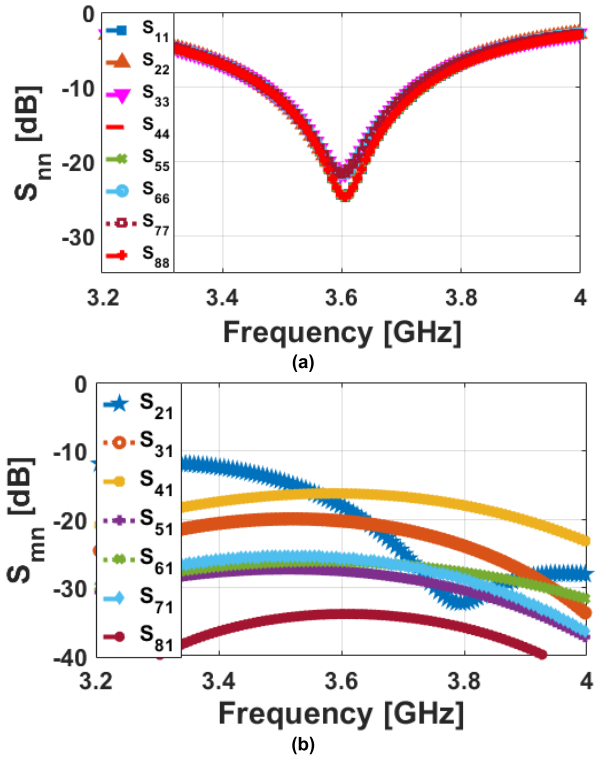

FIGURE 9. Simulated (a) S_{nn} and (b) S_{mn} of the MIMO array.

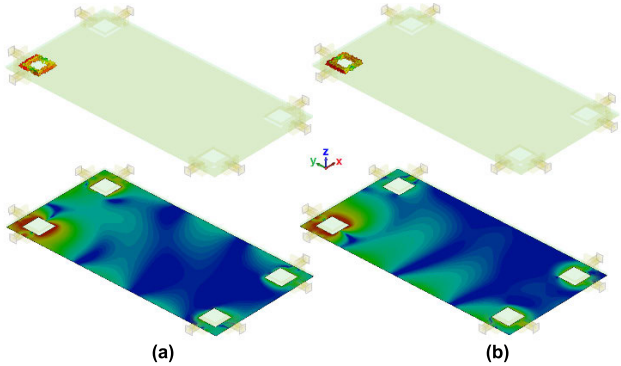

FIGURE 10. Current densities at 3.6 GHz for (a) 1st and (b) 2nd elements.

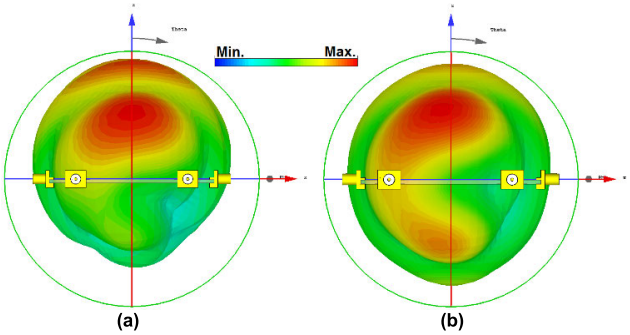

FIGURE 11. The radiation pattern of 1st antenna design (a) without, and (b) with the employed slot.

the 8-antenna system offers differently-polarized/high-gain radiations for the various regions of the smartphone board. Therefore, it can be concluded that the introduced array design could be robust with respect to the holding positions of the 5G smartphones. The efficiency properties are represented in Fig. 13. It can be seen that each antenna has a high radiation efficiency of more than 95%. They also exhibit better than 70% total efficiency at the 3.6 GHz resonance frequency. Moreover, as represented, for the range of 3.4-3.8 GHz, the obtained efficiencies are quite acceptable for MIMO smartphone operation [37], [38].

The proposed MIMO design has been prototyped and tested. The photo (front view with integrated SMA connectors) of the prototype sample is depicted in Fig. 14. The reflection/transmission coefficients of the representative antennas (S_{nn} and S_{mn}) of the array have been illustrated in Figs. 15 (a) and (b): the square-loop resonators offer well-defined results. In addition, the measurements are in good accordance with the simulations (Fig. 9) with sufficient impedance bandwidth and low couplings ≤ -17 dB. A very slight variation has been observed which might be due to the expected errors in prototyping, feeding the antennas, and also the experimental setup. It is worth mentioning the S_{21}

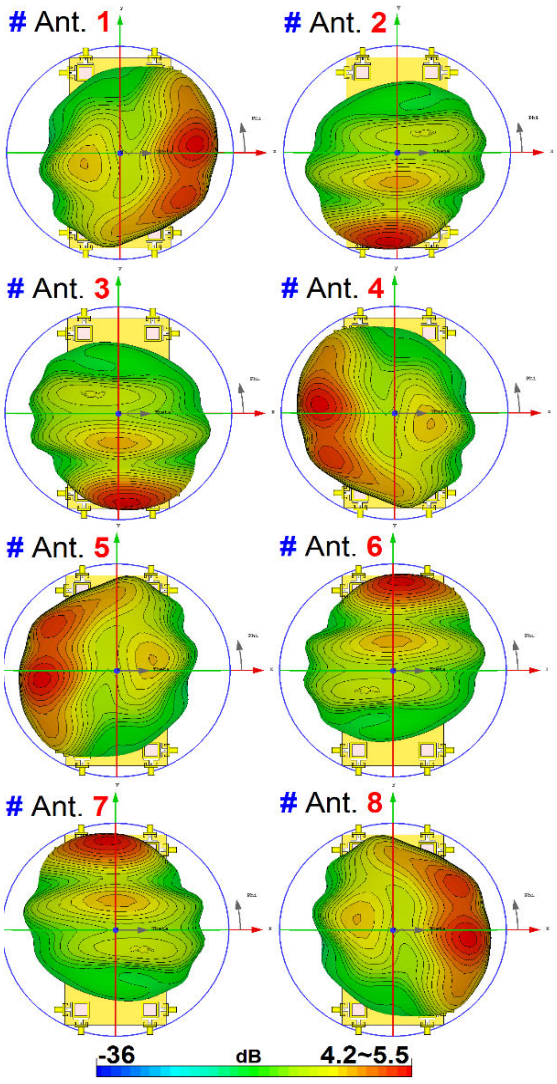

FIGURE 12. Radiation patterns of the antenna elements at 3.6 GHz.

characteristic of the main design differs slightly from the single antenna due to the large ground plane.

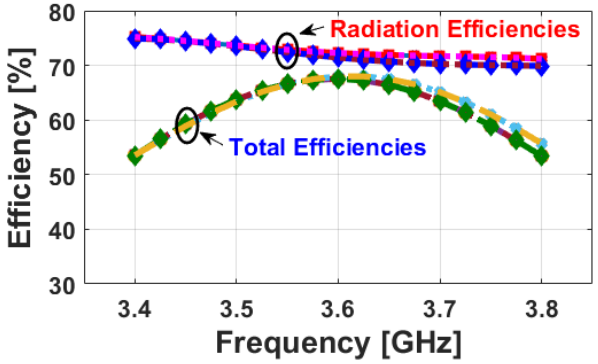

FIGURE 13. Radiation and total efficiencies of the design.

To verify the capability of the presented array in MIMO operation, the envelope correlation coefficient (ECC) and

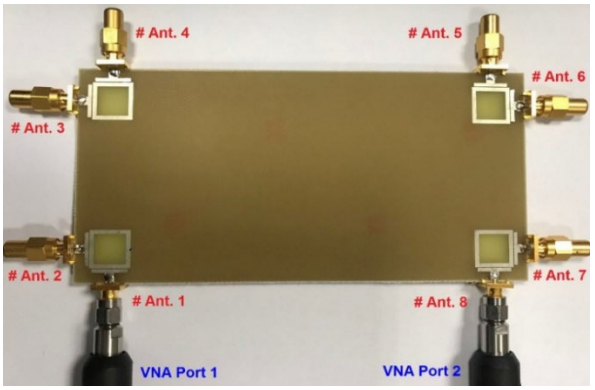

FIGURE 14. Fabricated smartphone antenna prototype.

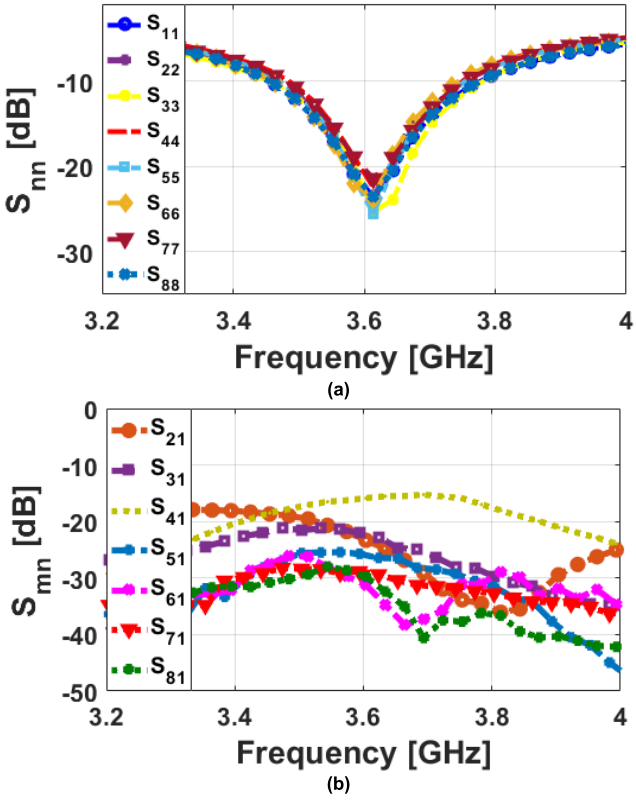

FIGURE 15. Measurement results for the (a) S_{nn} and (b) S_{mn} for the fabricated MIMO antenna sample.

total active reflection coefficient (TARC) properties of the fabricated MIMO smartphone antenna systems have been investigated and considered in the following (Fig. 16). It is worth mentioning that these parameters have been computed using the antenna S-parameters [39]. As represented, the results are very low (less than 0.004 and -30 dB at 3.6 GHz, respectively) in the band of interest. Owning to identical performances of the antenna pairs, radiations of the adjacent elements (Ants. 1 and 2) were investigated at 3.6 GHz and plotted in Fig. 16. As seen, the design exhibits desirable radiations that agreed well with the simulations. The corresponding elements also offer high gain.

TABLE 2. Comparison table of the introduced MIMO smartphone antenna.

Ref.	Antenna Type	Frequency (GHz)	Efficiency (%)	Gain (dBi)	Size (mm^2)	Isolation (dB)	ECC	Radiation Diversity
[11]	Coupled Monopole-Slot	2.6 GHz (2.55-2.65)	50-70	3	136 × 68	12	< 0.15	Yes
[12]	Fractal Monopole	3.5 GHz (3.4-3.6)	65-75	-	150×75	12	< 0.15	No
[13]	L-Shaped Strips	3.5 GHz (3.4-3.6)	50-5	4	136 × 68	15	< 0.10	No
[14]	I-Shaped Grounding	4.5 GHz (3.7-5.5)	-	4.5	140 × 68	15	< 0.40	Limited
[15]	Self-Isolated Element	3.5 GHz (3.4-3.6)	60-70	-	150×75	19	< 0.02	No
[16]	Balanced Open-Slot	3.5 GHz (3.4-3.6)	60-75	3.5	150×80	17	< 0.05	No
[17]	Communal Square-Loop	2.6 GHz (2.55-2.65)	45-60	2.5	136 × 68	12	< 0.20	Yes (Limited)
[18]	inverted-F antennas	3.5 GHz (3.4-3.6)	-	4	110 × 60	19	-	Yes (Limited)
[19]	quad-antenna linear (QAL)	3.5 GHz (3.4-3.6)	40-60	-	150×75	12	< 0.40	No
[20]	Loop Resonators	3.5 GHz (3.45-3.55)	35-50	2	145×70	16	< 0.20	No
[21]	open-end slot	3.5 GHz (3.4-3.6)	50-60	4.8	136 × 68	11	c<0.05	No
[22]	Self-complementary Ring Resonator	3.6 GHz (3.55-3.65)	50-70	4.5-6.2	150×75	12	-	Yes
[26]	H-shaped monopole	3.5 GHz (3.4-3.6)	60-70	2.8	150×75	11	<0.15	No
[27]	Mirrored Gap-Coupled Loop	(3.4-3.6) 3.5 GHz	40-60	-	150×75	12	< 0.20	No
[34]	Coaxial-Fed Patch	4.7 GHz (4.4-5)	40-80	5.5	150×80	12	< 0.20	No
[37]	Meandered-Dipoles	3.5 GHz (3.45-3.55)	48-67	-	144×74	15	< 0.10	No
[38]	Dual-Feed Module	3.5 GHz (3.45-3.55)	50-68	5.5	130 × 50	15	< 0.30	No
[39]	Half-Wavelength Shorted Loop	3.5 GHz (3.4-3.6)	50-78	4-5.8	150 × 77	10	< 0.1	No
[40]	Slot and Loop Antennas	3.5 GHz (3.4-3.6)	40-70	1.5-4.5	145 × 75	15	<0.15	No
[41]	L-Shaped Metal Strips	3.5 GHz (3.4-3.6)	40-70	5	150 × 63	10	< 0.1	No
[42]	Symmetric Dipole antenna	3.5 GHz (3.45-3.55)	50-70	-	154 × 74	15	< 0.1	No
This Work	**Diversity Loop Patch-Slot**	**3.6 GHz (3.4-3.8)**	**55-70**	**4.2-5.5**	**150×75**	**17**	**< 0.03**	**Yes Full-Coverage**

Table 2 represents the performance comparison between the introduced sub-6 GHz MIMO antenna array and those that have been reported in the literature. Fundamental properties such as employed element type, efficiency, gain, ECC, etc. are discussed. It is discovered that the developed antenna array has shown improved performance with sufficient characteristics. unlike most of the reported sub 6 GHz 5G antenna designs, the proposed antenna is in planar form with ease of integration and provides pattern and polarization diversity with full radiation coverage supporting different board's sides. It also provides high gains and radiation/total efficiencies. Furthermore, the array exhibits desirable performance in the presence of the user and smartphone components which will be discussed in the following.

IV. USER-IMPACT AND SAR ANALYSIS

This section discusses the user effects in terms of antenna efficiency performance and specific absorption rate (SAR) levels in the appearance of the user's hand and head phantoms [43]. Various usage postures have been considered in data/talk modes. Figures 18 and 19 depict the placements and the total efficiencies of the MIMO array in data-mode with the appearance of the single and double user-hand's phantoms with ε (permittivity)= 24 and σ (conductivity)= 2 s/m. As it is shown, the proposed smartphone antenna design exhibits sufficient performance for different data-mode scenarios touching the font/back layers of the mainboard.

However, some reductions in the efficiency levels of the elements have been observed. But still, the obtained

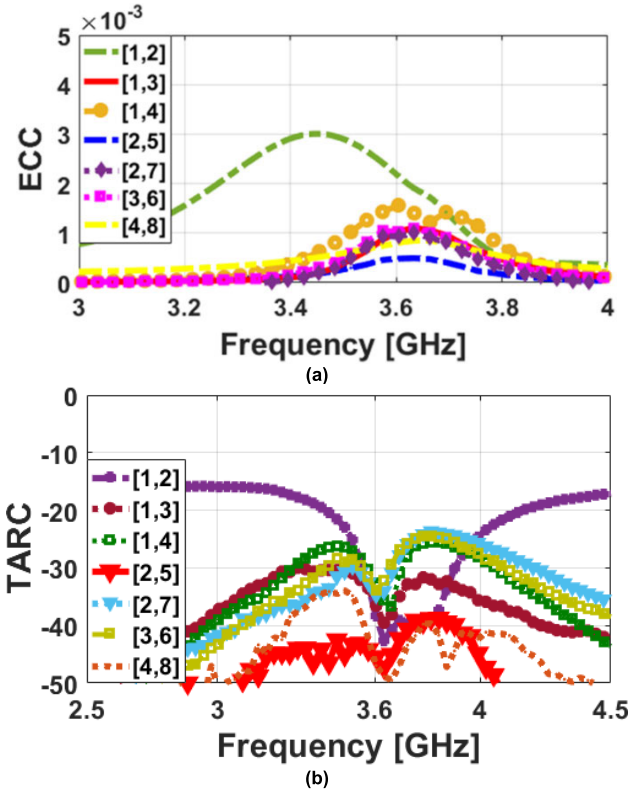

FIGURE 16. Calculated (a) ECC and (b) TARC results from measurements.

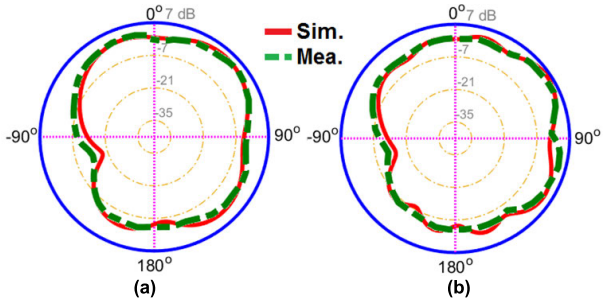

FIGURE 17. Radiation patterns at 3.6 GHz (a) 1st and (b) 2nd elements.

results are sufficient (around 50%) for MIMO and cellular applications. After careful investigation, it is realized that the highest losses of the antenna efficiencies are confirmed for the resonators partially surrounded by the hand phantoms. This is mainly due to the nature of the hand and head tissue, which usually absorbs the power of the radiation [15], [44], [45].

The 3D radiation patterns of each element in talk mode with the appearance of the user's hand/head are represented in Fig. 20. It is evident that the suggested MIMO smartphone antenna system offers well-defined radiation patterns with wide and full coverage supporting different regions. In addition, the elements provide acceptable gain levels in talk mode.

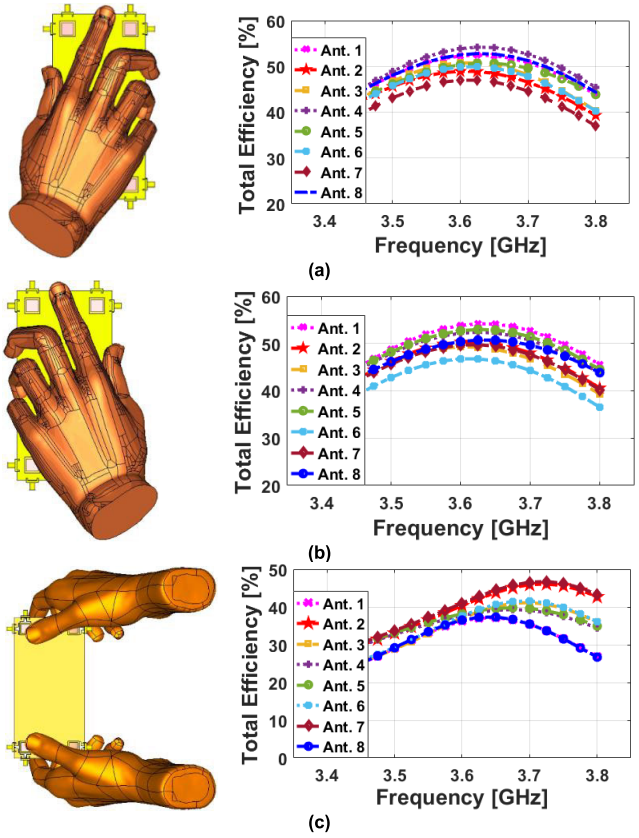

FIGURE 18. Placements and total efficiencies of the MIMO antenna elements in the presence of user hand for (a) right-hand, (b) left-hand, and (c) double-hand modes.

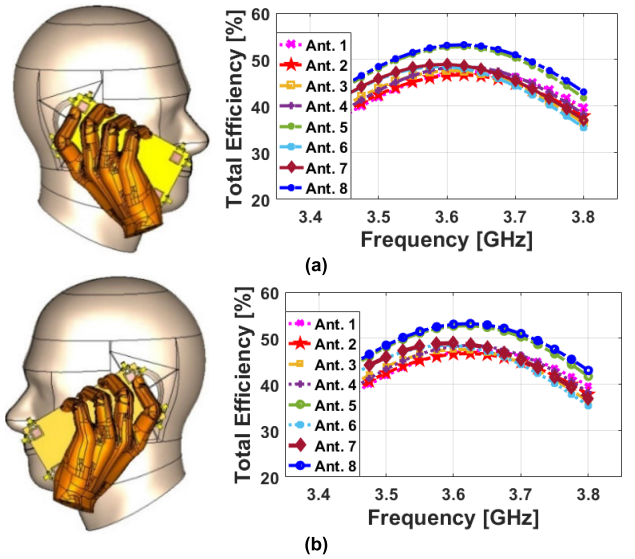

FIGURE 19. Placements and total efficiencies in talk-mode for (a) right-hand and (b) left-hand scenarios.

The specific absorption rate (SAR) distribution for the selected antenna elements in date-mode and talk-mode scenarios has been investigated and depicted in Figs. 21 and 22,

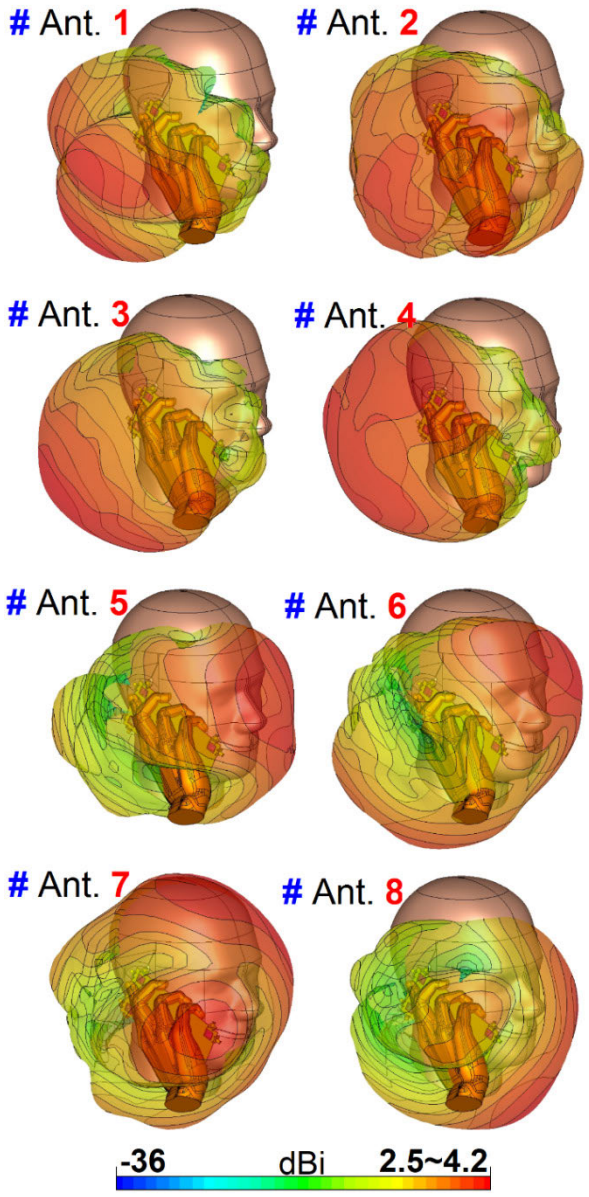

FIGURE 20. The array antenna radiations in Talk-Mode.

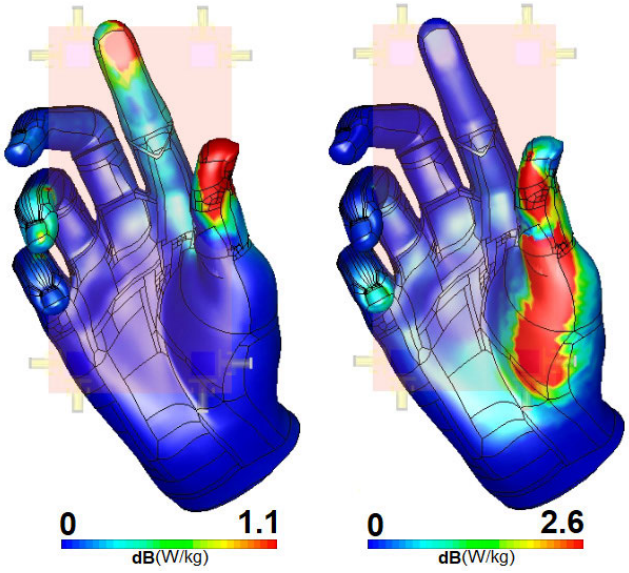

FIGURE 21. SAR Analysis of the proposed MIMO smartphone antenna design in data-mode for (a) Ant. 3 and (b) Ant. 6.

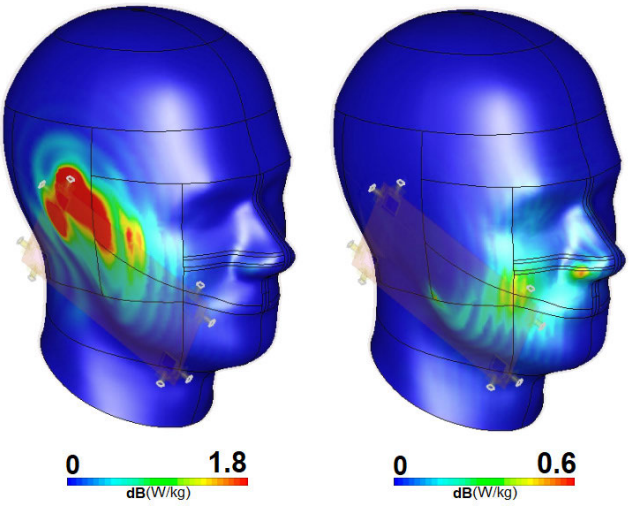

FIGURE 22. SAR Analysis of the proposed MIMO smartphone antenna design in talk-mode for (a) Ant. 2 and (b) Ant. 7.

respectively. For both scenarios, the elements with the highest and lowest SAR levels are represented. As shown in Fig. 21, for the data-mode scenario, it is discovered that Antenna 3 causes 1.1 dB (W/kg), the lowest SAR value while the highest value (2.6 dB (W/kg)) is observed from Antenna 6. Due to the array arrangement, it can be observed that the Antenna 2 is located slightly closer to the hand-phantom, compared to Antenna 6. The same conclusion could be applied to the talk mode. As shown in Fig. 22, In the talk-mode scenario, the maximum SAR level belongs to Antenna 2, and antenna 7 appears to have the minimum SAR value. Hence, it can be claimed that the closer the distance between the resonators and the phantom leads to the highest SAR level and vice versa [46], [47].

V. EFFECTS OF SMARTPHONE COMPONENTS

Another approach that should be considered for smartphone antennas is the antenna performance in the presence of the other components [48]. The integrated components could affect the overall performance of the designed antenna. Therefore, the placement, size, and orientation of the antenna elements are critical and need careful consideration. This section investigates the variation of the reflection coefficient characteristic for each element. The S_{nn}, reflection coefficient (S_{11} to S_{88}) results of the mobile-phone array structure in the vicinity of various integrated components such as the speaker, camera, LCD, battery, and USB connector have been considered and represented in Fig. 23. It has been discovered that the MIMO antenna design offers good S_{nn} operating

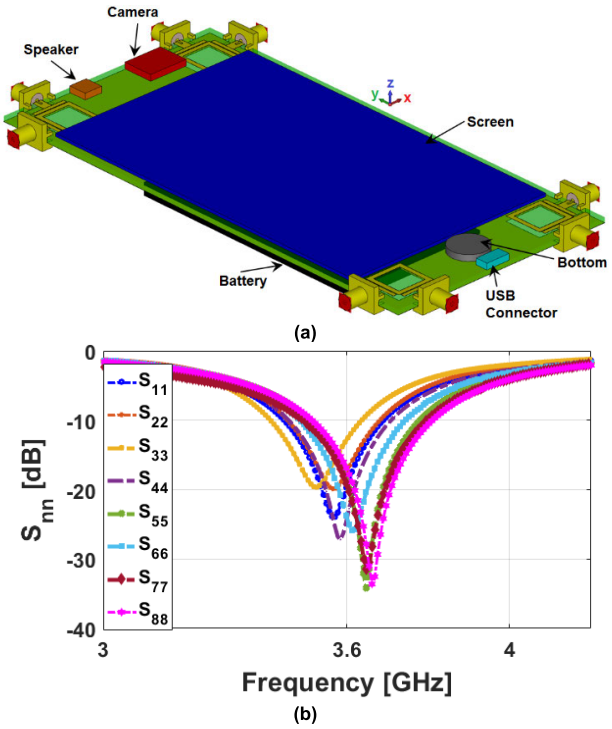

FIGURE 23. (a) Configuration and (b) reflection coefficients of the antenna system integrated with smartphone components.

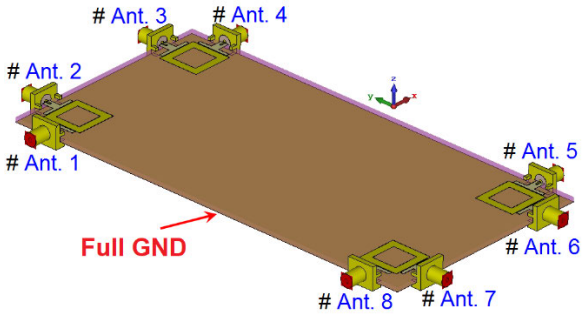

FIGURE 24. Configuration of the proposed MIMO smartphone antenna system with a full GND.

around 3.6 GHz bands with return loss lower than -20 dB. As depicted in Fig. 23 (b), the variations of the resonances are insignificant.

VI. MODIFIED DESIGN WITH A FULL GROUND PLANE

The performance of the proposed dual-polarized MIMO smartphone antenna with a full ground (GND) plane is studied in this section. As mentioned earlier, by modifying the configurations and slightly increasing the sizes of the employed dual-polarized radiators without the embedded slots in the ground plane, the proposed smartphone antenna is capable to operate at the target frequency of 3.6 GHz. In this case, the parameters of the square-loop radiation patch should be modified as follow: W_s = 26 mm, W= 14.5, W_1 = 9.3 mm. Other parameters

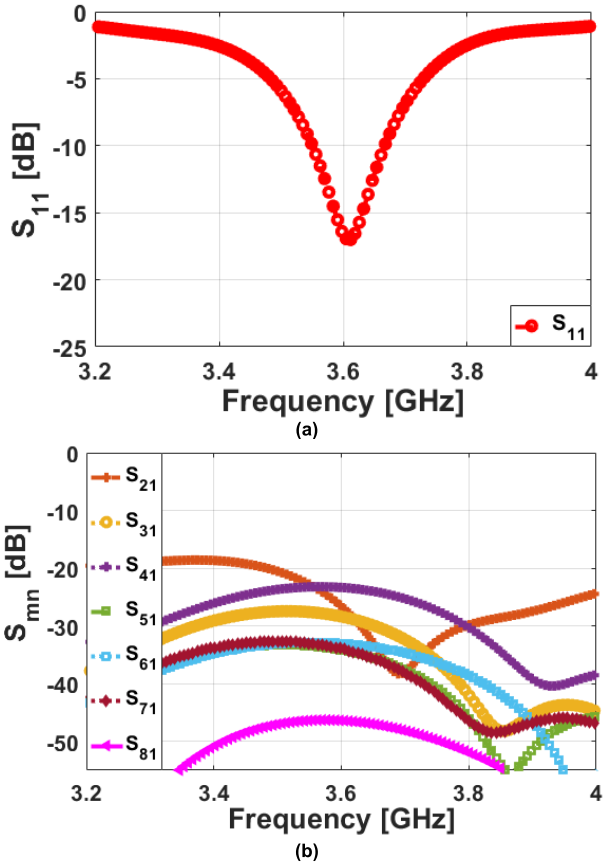

FIGURE 25. Simulated (a) S_{nn} and (b) S_{mn} of the modified MIMO array design with a full ground plane.

of the design remain unchanged including the overall size of the employed FR4 substrate, $W_{sub} \times Ls_{ub} \times h_{sub}$ =751× 50 × 1.6 mm^3.

Figure 24 represents the side view of the modified design with a full GND is represented which could give a possibility of a full-size screen integration. The S-parameters of the design with the full GND is shown in Fig. 25. As shown, the modified antenna elements provide sufficient S-parameters (S_{nn}/S_{mn}) at 3.6 GHz. However, compared to Fig. 8, the operation band is limited and covers less than 200 MHz bandwidth while better mutual coupling is observed. In addition, the radiation patterns of the antenna elements with full GND are provided in Fig. 26. As shown, unlike the proposed design, the radiating patterns of the elements mainly cover the top side of the PCB, which leads to reduced radiation coverage of the MIMO smartphone antenna [49].

VII. CONCLUSION

A dual-polarized eight-resonator array design formed by employing loop-slot structures is reported, with miniaturized elements working at the 3.6 GHz 5G band and proving wide impedance bandwidth. The presented MIMO design is simply constructed on a smartphone board with a low-cost and widely-used FR4 substrate material but meanwhile realizes

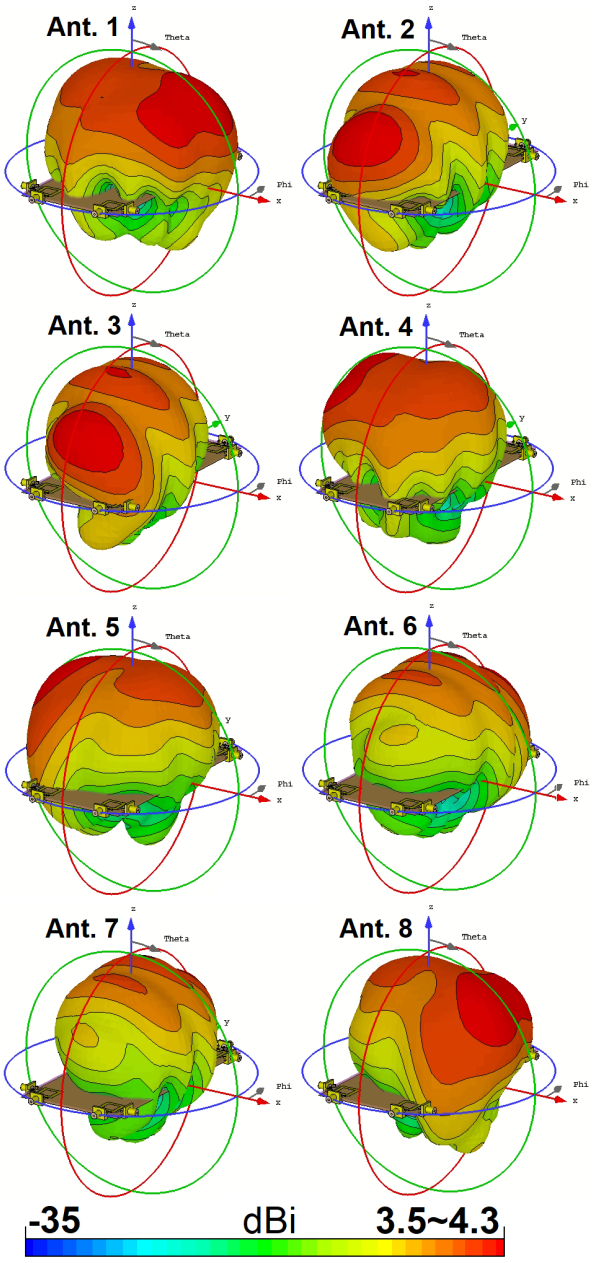

FIGURE 26. The radiation patterns of the modified MIMO antenna with a full GND at 3.6 GHz.

satisfactory properties. Acceptable characteristics in terms of input-impedance, mutual coupling, and diversity radiations are obtained. compared with recently reported designs, the suggested smartphone antenna design provides better gain/efficiency characteristics, improved radiation coverage, and lower ECC/TARC results. It also has a planar structure without any ohmic losses and is particularly a prospective candidate for future handheld platforms. Meanwhile, the integrated SAR levels and array performance in the appearance of the hand/head phantoms and smartphone components are discussed and quite acceptable results in terms of efficiency, reflection coefficient, and radiation coverage have been observed. Moreover, in order to confirm the accuracy of the designed MIMO smartphone antenna performances, the measurement results were carried out. The performance comparison showed quite good agreement for the simulation and experimental results. It is concluded that the desired gain levels and pattern diversity can be attained by suitably placing the proposed miniaturized resonators. Due to these attractive features, the proposed design can be used in future smartphones for high data-rate cellular communications

ACKNOWLEDGMENT

The authors extend their appreciation to the Deputyship for Research & Innovation, Ministry of Education in Saudi Arabia for funding this research work through project number RI-44-0421.

REFERENCES

[1] M. A. Jensen and J. W. Wallace, "A review of antennas and propagation for MIMO wireless communications," *IEEE Trans. Antennas Propag.*, vol. 52, no. 11, pp. 2810–2824, Nov. 2004.
[2] A. Osseiran, F. Boccardi, V. Braun, K. Kusume, P. Marsch, M. Maternia, O. Queseth, M. Schellmann, H. Schotten, H. Taoka, H. Tullberg, M. A. Uusitalo, B. Timus, and M. Fallgren, "Scenarios for 5G mobile and wireless communications: The vision of the METIS project," *IEEE Commun. Mag.*, vol. 52, no. 5, pp. 26–35, May 2014.
[3] F.-L. Luo and C. Zhang, "Massive MIMO for 5G: Theory, implementation and prototyping," in *Signal Processing for 5G: Algorithms and Implementations*. Piscataway, NJ, USA: IEEE, 2016, pp. 189–230.
[4] A. Yarali, "Fifth generation (5G) cellular technology," in *Public Safety Networks From LTE to 5G*. Hoboken, NJ, USA: Wiley, 2020, pp. 171–188.
[5] M. S. Sharawi, *Printed MIMO Antenna Engineering*. Norwood, MA, USA: Artech House, 2014.
[6] Z. Zhang, *Antenna Design for Mobile Devices*. Hoboken, NJ, USA: Wiley, 2011.
[7] N. O. Parchin, Y. I. A. Al-Yasir, and R. A. Abd-Alhameed, "A compact 5G antenna array with ultra-wide bandwidth for MM-wave smartphone applications," in *Proc. 15th Eur. Conf. Antennas Propag. (EuCAP)*, Mar. 2021, pp. 1–4.
[8] N. O. Parchin, J. Zhang, R. A. Abd-Alhameed, G. F. Pedersen, and S. Zhang, "A planar dual-polarized phased array with broad bandwidth and quasi-endfire radiation for 5G mobile handsets," *IEEE Trans. Antennas Propag.*, vol. 69, no. 10, pp. 6410–6419, Oct. 2021.
[9] A. Ullah, N. O. Parchin, A. S. I. Amar, and R. A. Abd-Alhameed, "Phased array antenna design with improved radiation characteristics for mobile handset applications," in *Proc. 16th Eur. Conf. Antennas Propag. (EuCAP)*, Mar. 2022, pp. 1–4.
[10] C.-C. Lin, C.-Y. Huang, and G.-H. Chen, "Obtuse pie-shaped quasi-self-complementary antenna for WLAN applications," *IEEE Antennas Wireless Propag. Lett.*, vol. 12, pp. 353–355, 2013.
[11] M.-Y. Li, Y.-L. Ban, Z.-Q. Xu, G. Wu, K. Kang, and Z.-F. Yu, "Eight-port orthogonally dual-polarized antenna array for 5G smartphone applications," *IEEE Trans. Antennas Propag.*, vol. 64, no. 9, pp. 3820–3830, Sep. 2016.
[12] M. Y. Muhsin, A. J. Salim, and J. K. Ali, "An eight-element MIMO antenna system for 5G mobile handsets," in *Proc. Int. Symp. Netw., Comput. Commun. (ISNCC)*, Oct. 2021, pp. 1–4.
[13] M. Abdullah, A. Altaf, M. R. Anjum, Z. A. Arain, A. A. Jamali, M. Alibakhshikenari, F. Falcone, and E. Limiti, "Future smartphone: MIMO antenna system for 5G mobile terminals," *IEEE Access*, vol. 9, pp. 91593–91603, 2021.
[14] C. Shi and Y. Sun, "A wideband six-port 5G MIMO mobile phone antenna," in *Proc. Int. Conf. Microw. Millim. Wave Technol. (ICMMT)*, May 2021, pp. 1–3.
[15] A. Zhao and Z. Ren, "Size reduction of self-isolated MIMO antenna system for 5G mobile phone applications," *IEEE Antennas Wireless Propag. Lett.*, vol. 18, no. 1, pp. 152–156, Jan. 2019.
[16] Y. Li, C.-Y.-D. Sim, Y. Luo, and G. Yang, "High-isolation 3.5 GHz eight-antenna MIMO array using balanced open-slot antenna element for 5G smartphones," *IEEE Trans. Antennas Propag.*, vol. 67, no. 6, pp. 3820–3830, Jun. 2019.

[17] M. Li, Z. Xu, Y. Ban, C. Sim, and Z. Yu, "Eight-port orthogonally dual-polarised MIMO antennas using loop structures for 5G smartphone," *IET Microw., Antennas Propag.*, vol. 11, no. 12, pp. 1810–1816, Sep. 2017.
[18] X. Zhao, S. P. Yeo, and L. C. Ong, "Decoupling of inverted-F antennas with high-order modes of ground plane for 5G mobile MIMO platform," *IEEE Trans. Antennas Propag.*, vol. 66, no. 9, pp. 4485–4495, Sep. 2018.
[19] K. L. Wong, J.-Y. Lu, L.-Y. Chen, W.-Y. Li, and Y.-L. Ban, "8-antenna and 16-antenna arrays using the quad-antenna linear array as a building block for the 3.5-GHz LTE MIMO operation in the smartphone," *Microw. Opt. Technol. Lett.*, vol. 58, no. 1, pp. 174–181, Jan. 2016.
[20] L.-Y. Rao and C.-J. Tsai, "8-loop antenna array in the 5 inches size smartphone for 5G communication the 3.4 GHz-3.6 GHz band MIMO operation," in *Proc. Prog. Electromagn. Res. Symp. (PIERS-Toyama)*, Aug. 2018, pp. 1995–1999.
[21] M. Abdullah, S. H. Kiani, L. F. Abdulrazak, A. Iqbal, M. A. Bashir, S. Khan, and S. Kim, "High-performance multiple-input multiple-output antenna system for 5G mobile terminals," *Electronics*, vol. 8, no. 10, p. 1090, Sep. 2019.
[22] N. O. Parchin, Y. I. A. Al-Yasir, J. M. Noras, and R. A. Abd-Alhameed, "Dual-polarized MIMO antenna array design using miniaturized self-complementary structures for 5G smartphone applications," in *Proc. 13th Eur. Conf. Antennas Propag. (EuCAP)*, 2019, pp. 1–4.
[23] *CST Microwave Studio*, Version 2020, CST, Framingham, MA, USA, 2020.
[24] S. P. Biswal, S. K. Sharma, and S. Das, "Collocated microstrip slot MIMO antennas for cellular bands along with 5G phased array antenna for user equipments (UEs)," *IEEE Access*, vol. 8, pp. 209138–209152, 2020.
[25] M. S. Sharawi, M. Ikram, and A. Shamim, "A two concentric slot loop based connected array MIMO antenna system for 4G/5G terminals," *IEEE Trans. Antennas Propag.*, vol. 65, no. 12, pp. 6679–6686, Dec. 2017.
[26] H. S. Kiani, A. Altaf, M. R. Anjum, S. Afridi, Z. A. Arain, S. Anwar, S. Khan, M. Alibakhshikenari, A. Lalbakhsh, M. A. Khan, R. A. Abd-Alhameed, and E. Limiti, "MIMO antenna system for modern 5G handheld devices with healthcare and high rate delivery," *Sensors*, vol. 21, no. 21, pp. 1–19, 2021.
[27] K.-L. Wong, C.-Y. Tsai, and J.-Y. Lu, "Two asymmetrically mirrored gap-coupled loop antennas as a compact building block for eight-antenna MIMO array in the future smartphone," *IEEE Trans. Antennas Propag.*, vol. 65, no. 4, pp. 1765–1778, Apr. 2017.
[28] C. E. Free and C. Aitchison, "RF and microwave antennas," in *RF and Microwave Circuit Design: Theory and Applications*. Hoboken, NJ, USA: Wiley, 2022, pp. 359–417.
[29] N. Takemura, A. Maruyama, and M. Hasegawa, "Inverted-FL antenna with self-complementary structure," in *Proc. IEEE Antennas Propag. Soc. Int. Symp.*, Jul. 2008, pp. 1–4.
[30] M. Alibakhshikenari, B. S. Virdee, P. Shukla, N. O. Parchin, L. Azpilicueta, C. H. See, R. A. Abd-Alhameed, F. Falcone, I. Huynen, T. A. Denidni, and E. Limiti, "Metamaterial-inspired antenna array for application in microwave breast imaging systems for tumor detection," *IEEE Access*, vol. 8, pp. 174667–174678, 2020.
[31] N. O. Parchin, Y. I. A. Al-Yasir, H. J. Basherlou, and R. A. Abd-Alhameed, "A closely spaced dual-band MIMO patch antenna with reduced mutual coupling for 4G/5G applications," *Prog. Electromagn. Res. C*, vol. 101, pp. 71–80, 2020.
[32] Y. I. A. Al-Yasir, N. O. Parchin, M. N. Fares, A. Abdulkhaleq, M. Sajedin, I. T. E. Elfergani, J. Rodriguez, and R. Abd-Alhameed, "New high-gain differential-fed dual-polarized filtering microstrip antenna for 5G applications," in *Proc. 14th Eur. Conf. Antennas Propag. (EuCAP)*, Mar. 2020, pp. 1–5.
[33] I. Elfergani, A. S. Hussaini, J. Rodriguez, and R. Abd-Alhameed, *Antenna Fundamentals for Legacy Mobile Applications and Beyond*. London, U.K.: Springer, 2017.
[34] A. Ullah, N. O. Parchin, M. Abdul-Al, H. M. D. Santos, C. H. See, Y. F. Hu, and R. A. Abd-Alhameed, "Internal MIMO antenna design for multi-band mobile handset applications," in *Proc. 29th Telecommun. Forum (TELFOR)*, 2021, pp. 1–4.
[35] H. H. Zhang, X. Z. Liu, G. S. Cheng, Y. Liu, G. M. Shi, and K. Li, "Low-SAR four-antenna MIMO array for 5G mobile phones based on the theory of characteristic modes of composite PEC-lossy dielectric structures," *IEEE Trans. Antennas Propag.*, vol. 70, no. 3, pp. 1623–1631, Mar. 2022.
[36] B. Cheng and Z. Du, "A wideband low-profile microstrip MIMO antenna for 5G mobile phones," *IEEE Trans. Antennas Propag.*, vol. 70, no. 2, pp. 1476–1481, Feb. 2022.
[37] W. A. E. Ali and A. A. Ibrahim, "A compact double-sided MIMO antenna with an improved isolation for UWB applications," *AEU-Int. J. Electron. Commun.*, vol. 82, pp. 7–13, Dec. 2017.
[38] S. H. Kiani, A. Iqbal, S.-W. Wong, H. S. Savci, M. Alibakhshikenari, and M. Dalarsson, "Multiple elements MIMO antenna system with broadband operation for 5th generation smart phones," *IEEE Access*, vol. 10, pp. 38446–38457, 2022.
[39] S. S. Alja'afreh, B. Altarawneh, M. H. Alshamaileh, E. R. Almajali, R. Hussain, M. S. Sharawi, L. Xing, and Q. Xu, "Ten antenna array using a small footprint capacitive-coupled-shorted loop antenna for 3.5 GHz 5G smartphone applications," *IEEE Access*, vol. 9, pp. 33796–33810, 2021.
[40] Y. Liu, A. Ren, H. Liu, H. Wang, and C.-Y. Sim, "Eight-port MIMO array using characteristic mode theory for 5G smartphone applications," *IEEE Access*, vol. 7, pp. 45679–45692, 2019.
[41] Y. Ye, X. Zhao, and J. Wang, "Compact high-isolated MIMO antenna module with chip capacitive decoupler for 5G mobile terminals," *IEEE Antennas Wireless Propag. Lett.*, vol. 21, no. 5, pp. 928–932, May 2022.
[42] H. H. Zhang, G. G. Yu, X. Z. Liu, G. S. Cheng, Y. X. Xu, Y. Liu, and G. M. Shi, "Low-SAR MIMO antenna array design using characteristic modes for 5G mobile phones," *IEEE Trans. Antennas Propag.*, vol. 70, no. 4, pp. 3052–3057, Apr. 2022.
[43] R. Khan, A. A. Al-Hadi, P. J. Soh, M. R. Kamarudin, M. T. Ali, and O. Owais, "User influence on mobile terminal antennas: A review of challenges and potential solution for 5G antennas," *IEEE Access*, vol. 6, pp. 77695–77715, 2018.
[44] M. Abdullah, S. H. Kiani, and A. Iqbal, "Eight element multiple-input multiple-output (MIMO) antenna for 5G mobile applications," *IEEE Access*, vol. 7, pp. 134488–134495, 2019.
[45] Z. Ji, Y. Guo, Y. He, L. Zhao, G.-L. Huang, C. Zhou, Q. Zhang, and W. Lin, "Low mutual coupling design for 5G MIMO antennas using multi-feed technology and its application on metal-rimmed mobile phones," *IEEE Access*, vol. 9, pp. 151023–151036, 2021.
[46] S. Xu, M. Zhang, H. Wen, and J. Wang, "Deep-subwavelength decoupling for MIMO antennas in mobile handsets with singular medium," *Sci. Rep.*, vol. 7, no. 1, p. 12162, Dec. 2017.
[47] M. Abdul-Al, A. S. I. Amar, I. Elfergani, R. Littlehales, N. O. Parchin, Y. Al-Yasir, C. H. See, D. Zhou, Z. Z. Abidin, M. Alibakhshikenari, C. Zebiri, F. Elmegri, M. Abusitta, A. Ullah, F. M. A. Abdussalam, J. Rodriguez, N. J. McEwan, J. M. Noras, R. Hodgetts, and R. A. Abd-Alhameed, "Wireless electromagnetic radiation assessment based on the specific absorption rate (SAR): A review case study," *Electronics*, vol. 11, no. 4, p. 511, Feb. 2022.
[48] M. H. Alshamaileh, S. S. Alja'afreh, and E. Almajali, "Nona-band, hybrid antenna for metal-rimmed smartphone applications," *IET Microw., Antennas Propag.*, vol. 13, pp. 2439–2448, Nov. 2019.
[49] S. K. Sharma and S. P. Biswal, "Multifunctional antennas for user equipments (UEs)," in *Multifunctional Antennas and Arrays for Wireless Communication Systems*. Piscataway, NJ, USA: IEEE, 2021, pp. 341–377.

NASER OJAROUDI PARCHIN (Senior Member, IEEE) received the Ph.D. degree in electrical engineering from the University of Bradford, U.K. He is currently an Assistant Professor (a Lecturer) at Edinburgh Napier University, U.K. He was a Postdoctoral Research Assistant at the Faculty of Engineering and Informatics, University of Bradford. He worked as a Research Fellow in the SATNEX V Project, funded by the European Space Agency. From 2018 to 2020, he was a Marie Curie Research Fellow in the H2020-ITN-SECRET Project, funded by EU Commission, targeting 5G mobile small cells. From 2014 to 2018, he worked with the APMS Section, Aalborg University, Denmark. In 2016, he was a Visiting Researcher at Ankara University, Turkey. He has over 12 years of research experience in antennas and microwave engineering. He is the author and the

coauthor of several books/book chapters and more than 300 technical journals and conference papers. His research interests include phased arrays, MIMO systems, smartphone antennas, SAR/user-impact, full-duplex diversity, 5G antennas, implementable and biomedical sensors, RFID tag antennas, millimeter-wave and terahertz components, fractal structures, metamaterials/metasurfaces, PCB realization, fabry resonators, EBG/FSS-inspired radiators, microwave filters, reconfigurable structures, and wireless propagation. He is a member of the Marie Curie Alumni Association (MCAA) and the European Association on Antennas and Propagation (EurAAP). He was a recipient and a co-recipient of various Awards and Grants for research publications, such as the 2018 Research Development Fund, 2020/2021 MDPI Travel Award, Best Paper Awards at URSI Symposium 2019, 5G Summit 2019, U.K. URSI Festival 2020, IMDC 2021, and ITC-Egypt 2022. He is a Research Grant Reviewer of the Dutch Science Council (NWO). He is also an Active Reviewer in various high-ranking journals and publishers, such as IEEE TRANSACTIONS, IEEE ACCESS/LETTERS, IET, Wiley, Springer, Elsevier, and MDPI. He is appointed as a guest editor and topic board of several MDPI journals. He was included in the World's Top Scientists list in 2016, 2020, 2021, and 2022. His papers have more than 6300 citations with 45 H-index, reported by Google Scholar. His score is higher than 95% of all RG members' scores.

AHMED S. I. AMAR received the bachelor's degree in electrical engineering from the University of Alexandria, Alexandria, Egypt, in 2008, and the master's and Ph.D. degrees in electrical engineering from Ain Shams University, Cairo, Egypt, in 2016 and 2022, respectively. He was an Honorary Research Fellow of radio frequency engineering at the Faculty of Engineering and Informatics, University of Bradford, Bradford, U.K., in 2021. He is currently a Researcher under MOD at the Electromagnetic Fields Department, ADR&D Center, Egypt, and a Lecturer with the Air Defense College, Egypt. His current research interests include antennas, RF and microwave circuit design, power amplifiers, RF system engineering, and millimeter-wave passive and active circuits design. He got the Best Paper Award at the International Telecommunications Conference (ITC-Egypt 2022).

MOHAMMAD DARWISH (Member, IEEE) received the B.Sc. (Hons.) and M.Sc. degrees in electrical engineering from the Military Technical College, Cairo, Egypt, in 2001 and 2008, respectively, and the Ph.D. degree in electrical engineering from the University of California, Davis, CA, USA, in 2013. Since then, he joined the Military Technical College, as an Assistant Professor, where he is currently the Head of the Radar Department. In 2019, he was a Visiting Scholar at the School of Electronic Engineering, Xidian University, Xi'an, China. His research interests include RF and microwave hybrid and integrated circuits, especially power amplifiers, antennas, and radars. His research also focuses on transceiver architectures and RF front-end performance enhancement for modern communication systems.

KARIM H. MOUSSA was born in Alexandria, Egypt, in 1984. He received the B.S., M.S., and Ph.D. degrees in electrical engineering (electronics and communications) from the Alexandria University, Alexandria, in 2006, 2011, and 2016, respectively. From 2016 to 2019, he was an Assistant Professor with the Ministry of Higher Education, Higher Institutes of Engineering and Technology, Communication Engineering Department. Since 2019, he has been an Assistant Professor with the Mechatronics Engineering Department, Horus University, Egypt, New Damietta, Egypt. He is currently an Assistant Professor with the School of Internet of Things, Xi'an Jiaotong-Liverpool University, Suzhou, China. He is the author of more than 15 articles. His research interests include advanced signal processing, advanced physical layer enhancement for next mobile generations, multimedia security, building smart adaptive algorithms, advanced-data coding/decoding techniques, and quantum cryptography.

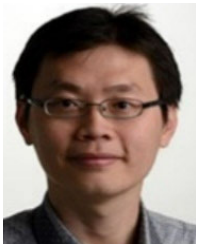

CHAN HWANG SEE (Senior Member, IEEE) received the B.Eng. degree (Hons.) in electronic, telecommunication and computer engineering and the Ph.D. degree from the University of Bradford, U.K., in 2002 and 2007, respectively. He was a Senior Research Fellow with the Antennas and Applied Electromagnetics Research Group, University of Bradford. He was a Senior Lecturer (a Program Leader) of electrical and electronic engineering with the School of Engineering, University of Bolton, U.K. He is currently an Associate Professor and the Head of electrical engineering and mathematics with the School of Engineering and the Built Environment, Edinburgh Napier University, U.K. He is also a Chartered Engineer. He has published over 100 peer-reviewed journal articles in below research areas. He has coauthored one book and three book chapters. His research interests include wireless sensor network system design, computational electromagnetism, antennas, microwave circuits, and acoustic sensor design. He is a fellow of the Institution of Engineering and Technology and the Higher Education Academy. He was a recipient of two Young Scientist Awards from the International Union of Radio Science (URSI) and Asia–Pacific Radio Science Conference (AP-RASC), in 2008 and 2010, respectively. He was awarded the Certificate of Excellence, for his successful knowledge transfer partnership (KTP) with Yorkshire Water, on the design and implementation of a wireless sensor system for sewerage infrastructure monitoring, in 2009. He is an Associate Editor for IEEE ACCESS and *PeerJ Computer Science* journals.

RAED A. ABD-ALHAMEED (Senior Member, IEEE) received the B.Sc. and M.Sc. degrees from the University of Basrah, Basrah, Iraq, in 1982 and 1985, respectively, and the Ph.D. degree from the University of Bradford, Bradford, U.K., in 1997, all in electrical engineering. Since September 2009, he has been a Research Visitor at Wrexham Glyndwr University, Wrexham, U.K., covering the wireless and communications research areas. He is currently a Leader of radiofrequency, propagation, sensor design, and signal processing; and Leads the Communications Research Group, for years at the School of Engineering and Informatics, Bradford University. He is also a Principal Investigator for several funded applications to EPSRCs and a Leader of several successful knowledge transfer programs (KTPs), such as Arris (previously known as Pace plc), Yorkshire Water plc, Harvard Engineering plc, IETG Ltd., Seven Technologies Group, Emkay Ltd., and Two World Ltd. He is a Professor of electromagnetic and radiofrequency engineering with the University of Bradford. He has also been a Co-Investigator in several funded research projects, including H2020 MARIE Sklodowska-CURIE ACTIONS: Innovative Training Networks "Secure Network Coding for Next Generation Mobile Small Cells

5G-US," nonlinear and demodulation mechanisms in biological tissue (Department of Health, Mobile Telecommunications, and Health Research Program, and Assessment of the Potential Direct Effects of Cellular Phones on the Nervous System (EU: collaboration with six other major research organizations across Europe). He has long years of research experience in the areas of radio frequency, signal processing, propagations, antennas, and electromagnetic computational techniques. He has published more than 500 academic journal articles and conference papers and has coauthored three books and several book chapters. His research interests include computational methods and optimizations, wireless and mobile communications, sensor design, EMC, beam steering antennas, energy-efficient PAs, and RF predistorter design applications. He is a fellow of the Institution of Engineering and Technology, U.K., and the Higher Education Academy. He is a Chartered Engineer, U.K. He received the Business Innovation Award for his successful KTP with Pace and Datong companies on the design and implementation of MIMO sensor systems and antenna array design for service localizations. He is the Chair of several successful workshops on Energy Efficient and Reconfigurable Transceivers: Approach Toward Energy Conservation and CO2 Reduction that addresses the biggest challenges for future wireless systems. He was appointed as a Guest Editor of *IET Science, Measurements and Technology*, in 2009 and 2012.

NORAH MUHAMMAD ALWADAI received the M.Sc. degree in solid state physics from King Saud University, Riyadh, Saudi Arabia, in 2012, and the Ph.D. degree in material science and engineering from the Semiconductor and Material Spectroscopy Group, King Abdullah University of Science and Technology (KAUST), Thuwal, in 2019. She is currently an Assistant Professor at the Physics Department, Princess Nourah Bint Abdulrahman University, Riyadh. Her research interests include semiconductor nanostructure (mainly ZnO and GaN related materials) functionalized by emerging materials for optoelectronic devices and microwave engineering. She received the Princess Nourah Bint Abdulrahman Award for research excellence for the university's scholarships and postgraduate studies, in 2020.

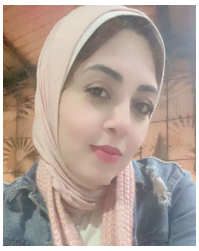

HEBA G. MOHAMED was born in Alexandria, Egypt, in 1984. She received the B.Sc. and M.Sc. degrees in electrical engineering from Arab Academy for Science and Technology, in 2007 and 2012, respectively, and the Ph.D. degree in electrical engineering from the University of Alexandria, Egypt, in 2016. In 2016, she was an Assistant Professor at the Alexandria Higher Institute of Engineering and Technology, Ministry of Higher Education, Egypt. Since 2019, she has been an Assistant Professor at the Faculty of Engineering, Communication Department, Princess Nourah Bint Abdulrahman University, Saudi Arabia. Her research interests include cryptography, wireless communication, mobile data communication, the Internet of Things, and computer vision.